



OPEN

## Inhibition of miR-194-5p avoids DUSP9 downregulation thus limiting sepsis-induced cardiomyopathy

Jie Wang<sup>1,2</sup>, Ting Wei<sup>1,2</sup>, Wei Zhang<sup>1</sup>, Yi Chu<sup>1</sup>, Dongwei Zhang<sup>1</sup>, Mingming Zhang<sup>1</sup>, Jianqiang Hu<sup>1</sup>, Zhaole Ji<sup>1</sup>✉ & Qimeng Hao<sup>1</sup>✉

Sepsis-induced cardiomyopathy (SIC) is described as a reversible myocardial depression that occurs in patients with septic shock. Increasing evidence shows that microRNA-194-5p (miR-194-5p) participates in the regulation of oxidative stress, mitochondrial dysfunction, and apoptosis and its expression is associated with the occurrence and progression of cardiovascular disease; however, the effects of miR-194-5p in SIC are still unclear. This study explores whether miR-194-5p could modulate SIC by affecting oxidative stress, mitochondrial function, and apoptosis. Experimental septic mice were induced by intraperitoneal injection of lipopolysaccharide (LPS) in C57BL/6J mice. The biological role of miR-194-5p in SIC in vivo was investigated using cardiac echocardiography, ELISA, western blot, qRT-PCR, transmission electron microscopy, terminal deoxynucleotidyl transferase dUTP nick end labeling (TUNEL) assay, bioinformatics analysis, and dual-luciferase reporter gene assay. Our major finding is that miR-194-5p antagomir mitigates sepsis-induced cardiac dysfunction, inflammation, oxidative stress, apoptosis and mitochondrial dysfunction in the hearts of septic mice, while miR-194-5p agomir triggers the opposite effects. Furthermore, dual-specificity phosphatase 9 (DUSP9) is a direct target of miR-194-5p and the cardioprotective effects of miR-194-5p antagomir on cardiac dysfunction, inflammation, apoptosis, mitochondrial dysfunction and oxidative stress are abolished through inhibiting DUSP9. Therefore, miR-194-5p inhibition could mitigate SIC via DUSP9 in vivo and the novel miR-194-5p/DUSP9 axis might be the potential treatment targets for SIC patients.

**Keywords** MicroRNA-194-5p, Sepsis-induced cardiomyopathy, Dual-specificity phosphatase 9, Mitogen-activated protein kinases, Lipopolysaccharide

Sepsis, induced by a maladjusted host response to infection, is a life-threatening organ dysfunction and an increasingly severe global health burden<sup>1</sup>. It is estimated that 18 million patients worldwide are infected with sepsis, which is one of the leading causes of death in critically ill patients<sup>2</sup>. Although the treatment of sepsis has improved significantly in the past few years, sepsis incidence and mortality are still increasing<sup>3</sup>. Sepsis-induced cardiomyopathy (SIC) is a common complication of sepsis and the typical clinical manifestations of SIC are ventricular dilatation, reduced ventricular contractility and/or decreased volume resuscitation response<sup>4</sup>. It is a reversible myocardial depression and many myocardial depressant factors have been identified including oxidative stress, mitochondrial dysfunction, dysregulation of inflammatory mediators, endothelial dysfunction, abnormal calcium movement within cells, myocyte apoptosis, and autonomic dysregulation<sup>5</sup>. Despite advances in intensive care and supportive technology to prevent the progression of SIC, these strategies are often disappointing and the pathogenesis of SIC is still unclear. Therefore, it is urgent to find new therapeutic targets to protect against cardiac injury caused by sepsis.

MicroRNAs (miRNAs) are endogenous small noncoding RNAs that regulate gene expression by binding to the 3'-untranslated region (3'-UTR) of target mRNAs to inhibit translation or induce mRNA degradation and, therefore, are involved in various physiological and pathophysiological processes, such as proliferation, cell death, migration, and differentiation<sup>6–8</sup>. Growing evidence indicates that miRNAs play vital roles in the maintenance of normal heart development and are involved in the etiology and pathogenesis of cardiovascular diseases,

<sup>1</sup>Department of Cardiology, Tangdu Hospital, Air Force Medical University, Xi'an 710032, Shaanxi, China. <sup>2</sup>These authors contributed equally: Jie Wang and Ting Wei. ✉email: jizhaole@163.com; fireman1@fmmu.edu.cn

including SIC<sup>9,10</sup>. Recent studies have revealed that the serum level of miR-194 is significantly increased both in patients with heart failure within one year after acute myocardial infarction and in patients suffering from obese cardiomyopathy, and the level of circulating miR-194 is positively correlated with cardiac dysfunction<sup>11,12</sup>. Although currently the regulatory mechanism of miR-194 production is still poorly clarified, the changes in miR-194 level may indicate a pathophysiological condition. Furthermore, obese mice-original circulating exosomal miR-194 can dampen mitochondrial function in mouse cardiomyocytes, while miR-194 sponge, a specific inhibitor, can effectively reverse the mitochondrial inhibitory effect from obese mice-original exosomes<sup>12</sup>. More interestingly, miR-194 inhibitor can protect against obesity-induced cardiac dysfunction, structural disorders and mitochondrial inactivity<sup>12</sup>. Besides, miR-194-5p has been reported to be involved in the regulation of apoptosis and endoplasmic reticulum stress in doxorubicin-induced cardiotoxicity model and silencing of miR-194-5p can improve DOX-induced cardiac dysfunction<sup>13</sup>. Although accumulating evidence indicates that miR-194-5p may exert protective cardiovascular effects, the physiological role of miR-194-5p in SIC is currently poorly elucidated.

Dual-specificity phosphatase 9 (DUSP9), also known as MAP kinase phosphatase-4 (MKP-4), belongs to the threonine/tyrosine dual-specific phosphatase family<sup>14</sup>. DUSP9 plays a vital role in human diseases, including cancer, myocardial injury, diabetes, obesity, and liver metabolic syndromes<sup>14</sup>. It can dephosphorylate mitogen-activated protein kinases (MAPK), including JNK, p38, and ERK1/2, resulting in the negative control of MAPK signal transduction, which is closely associated with the development of cardiovascular disease<sup>14</sup>. Previous studies indicate DUSP9 overexpression attenuates cardiac hypertrophy in mice<sup>15</sup>. DUSP9 may be a crucial factor involved in the progression of cardiovascular disease. However, the role of DUSP9 in SIC is currently poorly understood.

In the present study, we investigated the potential role of miR-194-5p in lipopolysaccharide (LPS)-induced myocardial injury. Our results demonstrated that miR-194-5p was upregulated in the hearts of septic mice compared to normal controls. Mechanistically, knockdown or overexpression of miR-194-5p led to improved or deteriorated cardiac function in mice with sepsis, respectively. In addition, miR-194-5p targeted DUSP9 and inhibited its expression. These findings suggest that the novel miR-194-5p/DUSP9 axis might be the potential treatment targets for SIC patients.

## Materials and methods

### Experimental animals

Eight-week-old C57BL/6 male mice were purchased from the Laboratory Animal Center of the Air Force Medical University. All procedures were approved by the Institutional Animal Care and Use Committee of the Fourth Military Medical University following Animal Research: Reporting of In Vivo Experiments (ARRIVE) guidelines and conformed to the Guide for the Care and Use of Laboratory Animals published by the National Institutes of Health.

### Experimental protocol

The experimental mice were randomly allocated into the following groups (25 mice in each group): The control group (control), the LPS group (LPS), the LPS + antagomir control group (LPS + antagomir control), the LPS + miR-194-5p antagomir group (LPS + miR-194-5p antagomir), the LPS + agomir control group (LPS + agomir control) and the LPS + miR-194-5p agomir group (LPS + miR-194-5p agomir). To explore whether miR-194-5p regulates LPS-induced myocardial injury via targeting DUSP9, mice were allocated to the following groups (25 mice in each group): (1) the LPS + shControl group (LPS + shCtrl); (2) the LPS + shDUSP9 group (LPS + shDUSP9); (3) the LPS + miR-194-5p antagomir (LPS + miR-194-5p antagomir) and (4) the LPS + miR-194-5p antagomir + shDUSP9 group (LPS + miR-194-5p antagomir + shDUSP9). Modified miR-194-5p agomir and antagomir were synthesized by GenePharma (Shanghai, China), which were used to increase and decrease miR-194-5p expression *in vivo*, respectively. Agomir control and antagomir control are non-functional double-stranded RNAs and single-stranded RNAs with unrelated sequences, respectively. MiR-194-5p agomir (10 mg/kg each time), antagomir (10 mg/kg each time), and a comparable dose of negative control (agomir control or antagomir control), were dissolved with RNase-free PBS and injected through tail vein twice weekly for 3 weeks prior to LPS injection. The dose of the agomir/antagomir we used was referring to the previous study<sup>16</sup> and the introduction manuals of the miR-194-5p agomir/antagomir. Adeno-associated virus serotype 9 (AAV9) carrying cardiac troponin T (cTnT) promoter-driven small hairpin RNA targeting DUSP9 (shDUSP9) or negative control (shCtrl) were generated by Hanbio Biotechnology (Shanghai, China) and 50  $\mu$ l of  $2 \times 10^{11}$  IU/ml viral particles per mouse were injected via tail vein 3 weeks prior to LPS injection. LPS (Cat. No. SMB00704; Sigma-Aldrich) was used to establish animal model. LPS (10 mg/kg) was dissolved in normal saline and administered through intraperitoneal injection. Levels of miR-194-5p, DUSP9, p-p38, p38, p-JNK and JNK expression in heart tissue were measured by using RT-qPCR and western blot at 0 h, 6 h, 12 h, 18 h and 24 h after LPS injection. The remaining experiments were implemented at 24 h after LPS injection.

### Echocardiography and measurement of cardiac hemodynamics

Cardiac echocardiography was performed by using an echocardiogram (15.0 MHz, VisualSonics Vevo 2100) after anesthesia to evaluate the changes in left ventricular end-diastolic dimension (LVEDD), left ventricular end-systolic dimension (LVESD), left ventricular ejection fraction (LVEF) and left ventricular fraction shortening (LVFS). The systolic pressure of left ventricular (LVSP) and end-diastolic pressure of left ventricular (LVEDP) were measured by Millar Mikro-tip catheter sensor and hemodynamic indexes were calculated. The first derivative of left ventricular pressure ( $\pm$  LV dp/dt max) was measured and evaluated by computer algorithms and an interactive video camera program (Po-Ne-Mah Physiology Platform P3 Plus, Gould Instrument Systems).

### Measurement of tissue interleukin (IL)-1 $\beta$ , IL-6 and tumor necrosis factor (TNF)- $\alpha$ concentrations

The concentrations of IL-1 $\beta$  (Cat. No. H002-1-2; Nanjing Jiancheng Bioengineering Institute), IL-6 (Cat. No. H007-1-2; Nanjing Jiancheng Bioengineering Institute) and TNF- $\alpha$  (Cat. No. H052-1-2; Nanjing Jiancheng Bioengineering Institute) in the heart tissue were evaluated using commercially available ELISA kits according to the instructions of the kits, respectively.

### Transmission electron microscopy

The mice were anaesthetized using inhalational isoflurane (1.5%). The hearts were harvested and the blood of the hearts was washed off with PBS on wet ice. The left ventricular myocardium was cut into 1 mm cubes and fixed in 2% glutaraldehyde. The specimens were graded dehydrated, embedded, solidified, sliced and double stained with 3% uranium acetate and lead citrate. The images were observed by a JEOL JEM-2000EX transmission electron microscope (JEOL, Ltd.). Five fields were randomly selected and photographed. The pictures were analyzed by two technicians blinded to the study.

### Isolation of mitochondria

A cell mitochondria isolation kit (Cat. No. G006-1-1; Nanjing Jiancheng Bioengineering Institute) was used to isolate mitochondria from hearts as previously described<sup>17</sup>.

### Determination of ATP content and citrate synthase

An ATP assay kit (Cat. No. S0026; Beyotime Institute of Biotechnology) was employed to assess the ATP content of heart tissues. Citrate synthase (CS) was evaluated using the CS Assay kit (Cat. No. 232-821-7; Sigma-Aldrich) according to the instructions of the kit.

### Determination of mitochondrial calcium retention capacity (mCRC)

The mCRC indicates the ability of mitochondria to absorb calcium before permeability transition. The detection method of mCRC was previously described in the literature<sup>17</sup>.

### Estimation of malondialdehyde (MDA) and reactive oxygen species (ROS) production in heart tissue

The levels of MDA and ROS were measured using MDA assay kit (Cat. No. S0131S; Beyotime Institute of Biotechnology) and ROS assay kit (Cat. No. E004-1-1; Nanjing Jiancheng Bioengineering Institute) according to the protocols of the kits, respectively.

### Western blot analysis

The hearts were quickly removed and the blood was washed off with pre-cooled PBS. The heart tissues were lysed with RIPA lysate containing a protease inhibitor cocktail (Cat. No. P0013B; Beyotime Institute of Biotechnology). A BCA protein assay kit (Cat. No. A045-4-2; Nanjing Jiancheng Bioengineering Institute) was used to quantify protein concentration. Following protein electrophoresis and transfer, the membranes were blocked, and incubated with primary antibodies overnight. These full-length membranes were not cut prior to hybridization with antibodies. The membranes were incubated with HRP-conjugated secondary antibodies the next day and the bands were detected by a chemiluminescence system (Bio-Rad). ImageJ software was employed to analyze protein expression<sup>18</sup>.

### RNA extraction and quantitative real-time PCR

The total RNA of tissues was extracted by homogenization in RNAiso Plus (Takara, Japan). The level of miR-194-5p was quantified using the stem-loop RT-qPCR method. A quantitative real-time PCR assay was performed with SYBR Premix ExTaq (Cat. No. DRR041A; Takara) on a CFX96 real-time PCR operating system (Bio-Rad, Hercules, CA, USA) using the cDNA as the template. The reaction conditions were defined as follows: a pre-denaturation step at 95 °C for 10 s, and 40 cycles of 95 °C for 15 s, 60 °C for 30 s, and 72 °C for 60 s. The expression level of miRNA was normalized to U6 was used as an internal control for mRNA. The comparative 2<sup>- $\Delta\Delta$ Ct</sup> method was used to analyze the gene expression levels. The primer sequences for qPCR were as follows: miR-194-5p Forward: 5'-CGCGTGTAACAGCAACTCCA-3' and Reverse: 5'-AGTGCAGGGTCCGAGGTTT-3'; U6 Forward: 5'-ATTGGAACGATACAGAGAAGATT-3' and Reverse: 5'-GGAACGCTTCACGAATTTG-3'.

### Reagents and antibodies

The following primary antibodies were used: JNK (1:1000; Cat. No. #9252; Cell Signaling Technology, Inc.), phosphorylated (p)-JNK (Thr183/ Thr185) (1:1000; Cat. No. #9255; Cell Signaling Technology, Inc.), p38 (1:1000; Cat. No. #8690; Cell Signaling Technology, Inc.), p-p38 (Thr180/ Thr182) (1:1000; Cat. No. #4511; Cell Signaling Technology, Inc.), p65 (1:1000; Cat. No. #8242; Cell Signaling Technology, Inc.), p-p65 (Ser536) (1:1000; Cat. No. #3033; Cell Signaling Technology, Inc.), Jak2 (1:500; Cat. No. ab108596; Abcam, Inc.), p-Jak2 (Tyr1007/ Tyr1008) (1:500; Cat. No. ab32101; Abcam, Inc.), Stat3 (1:500; Cat. No. ab68153; Abcam, Inc.), p-Stat3 (Tyr705) (1:500; Cat. No. ab267373; Abcam, Inc.), DUSP9 (1:1000; Cat. No. 26718-1-AP; Proteintech, Wuhan, China) and GAPDH (1:5000; Cat. No. sc-32233; Santa Cruz, Biotechnology, Inc.). HRP-conjugated secondary antibody (anti-rabbit IgG) (1:5000; Cat. No. 15015; Proteintech) were used.

### Examination of cardiac apoptosis

Cardiac apoptosis was evaluated by using a TUNEL assay kit (Cat. No. C10617; Thermo Fisher Scientific) as described previously<sup>17</sup>. Heart sections were incubated with fluorescein-dUTP in a humid chamber for 1 h and the apoptotic cell nuclei were stained by DAPI (Cat. No. D9542; Sigma-Aldrich). Five visual fields under the confocal microscope were selected randomly and then an average apoptosis index was calculated by dividing the number of Troponin I/TUNEL-positive cells by the total number of Troponin I/DAPI-positive cells in each group.

### Determination of caspase-3 and caspase-9 activity

The activities of caspase-3 and caspase-9 in the heart tissue were evaluated using the Caspase-3 Activity Assay kit (Cat. No. C1116; Beyotime) and Caspase-9 Activity Assay kit (Cat. No. C1158; Beyotime) according to the manufacturer's protocols. Briefly, after homogenization of the heart tissue in cell lysis buffer, homogenates were centrifuged for 15 min at 12,000 × g, and the supernatant (100 µg protein) was incubated with reaction buffer containing Ac-DEVD-pNA (caspase-3 substrate) or Ac-LEHD-pNA (caspase-9 substrate). After further incubation at 37 °C for 4 h, the release of p-nitroanilide (pNA) was evaluated by measuring the absorbance at a wavelength of 405 nm using a microplate reader. The activities of caspase-3 and caspase-9 were expressed relative to the control sample.

### Dual-luciferase reporter gene assay

The 3'-UTR of DUSP9 was constructed and cloned downstream of the luciferase gene into the luciferase reporter vector pGL3 (Promega, WI, USA). A mutant 3'-UTR of DUSP9 was constructed using the Quick Change II XL Site-Directed Mutagenesis Kit (Agilent Technologies, USA). HEK-293T cells were cultured at 85% confluence and transfected with miR-194-5p mimics or mimic control (20 pmol) along with the luciferase reporter gene construct (DUSP9-3'UTR and Mut-DUSP9-3'UTR, 100 ng) using Lipofectamine 3000 (Cat. No. L3000008; Invitrogen). The luciferase activity was determined using the Glomax20/20 luminometer (Promega) and the luciferase assay kits (cat. no. 11402ES60; Yeasen Bioengineering Institute).

### Statistical analysis

Data are expressed as means ± standard deviation (SD). The differences between multiple groups were evaluated using one-way analysis of variance followed by the Student–Newman–Keuls test. *P* values < 0.05 was considered to indicate a statistically significant difference.

## Results

### MiR-194-5p antagomir improves, whereas miR-194-5p agomir deteriorates cardiac function and inflammation in septic mice

To investigate the implication of miR-194-5p in LPS-induced cardiac dysfunction, miR-194-5p expression was measured at 0 h, 6 h, 12 h, 18 h and 24 h after LPS injection (Fig. 1a). Time-dependent upregulation in mRNA expression of miR-194-5p was detected in the septic myocardium, which may indicate that miR-194-5p may be involved in LPS-induced myocardial injury. Knockdown and overexpression efficiency of miR-194-5p at the mRNA level were confirmed by qRT-PCR (Fig. 1b). As revealed by echocardiography and cardiac hemodynamics parameters, significantly increased LVEDD, LVESD, and LVEDP, and decreased LVEF, LVFS, LVSP, and ± LV dp/dt were observed in the septic myocardium compared with in the control myocardium (Fig. 1c). The treatment of miR-194-5p antagomir reduced the levels of LVEDD, LVESD, and LVEDP, and augmented the levels of LVEF, LVFS, LVSP, and ± LV dp/dt in the septic myocardium. On the contrary, the delivery of miR-194-5p agomir exhibited opposite effect as evidenced by increased levels of LVEDD, LVESD, and LVEDP. It decreased levels of LVEF, LVFS, LVSP, and ± LV dp/dt in the septic myocardium (Fig. 1d–i; Supplement Fig. 1a,b).

Inflammatory response is the central link of SIC, and therefore, the effects of miR-194-5p on the inflammatory response in septic myocardium were evaluated. Compared with the LPS group, IL-1β, IL-6 and TNF-α were significantly decreased in the miR-194-5p antagomir group while increased in the miR-194-5p agomir group (Fig. 1j–l). In SIC, the activation of NFκB pathway and Jak2/Stat3 pathway may be critical mechanisms involved in the release of IL-1β, IL-6 and TNF-α in septic myocardium. Compared with the LPS group, p-p65/p65 ratio was significantly decreased in the miR-194-5p antagomir group while increased in the miR-194-5p agomir group. Interestingly, no significant changes in p-Jak2/Jak2 and p-Stat3/Stat3 ratios were observed in either miR-194-5p antagomir group or miR-194-5p agomir group compared with in the LPS group (Supplement Fig. 2a–d). These results indicate that miR-194-5p antagomir relieves, whereas miR-194-5p agomir exacerbates inflammation in mice with LPS-induced sepsis by regulating the NFκB pathway.

### MiR-194-5p antagomir mitigates, whereas miR-194-5p agomir aggravates cardiac apoptosis in hearts from sepsis-challenged mice

The effects of miR-194-5p on cardiac apoptosis were probed by the TUNEL assay (Fig. 2a). More TUNEL-positive cells were observed in the septic myocardium compared with in the control myocardium. TUNEL-positive cells were decreased by miR-194-5p antagomir treatment, whereas they increased by miR-194-5p agomir administration in the septic myocardium (Fig. 2a,b). The effects of miR-194-5p on caspase activities were also explored (Fig. 2c,d). Higher levels of caspase-3 and caspase-9 activities were detected in the septic myocardium compared with in the control myocardium. MiR-194-5p antagomir treatment decreased caspase-3 and caspase-9 activities, whereas miR-194-5p agomir administration exerted an opposite role in the septic myocardium. These results indicate that miR-194-5p is involved in cardiac apoptosis in SIC, which may be mediated through the caspase-dependent pathway.

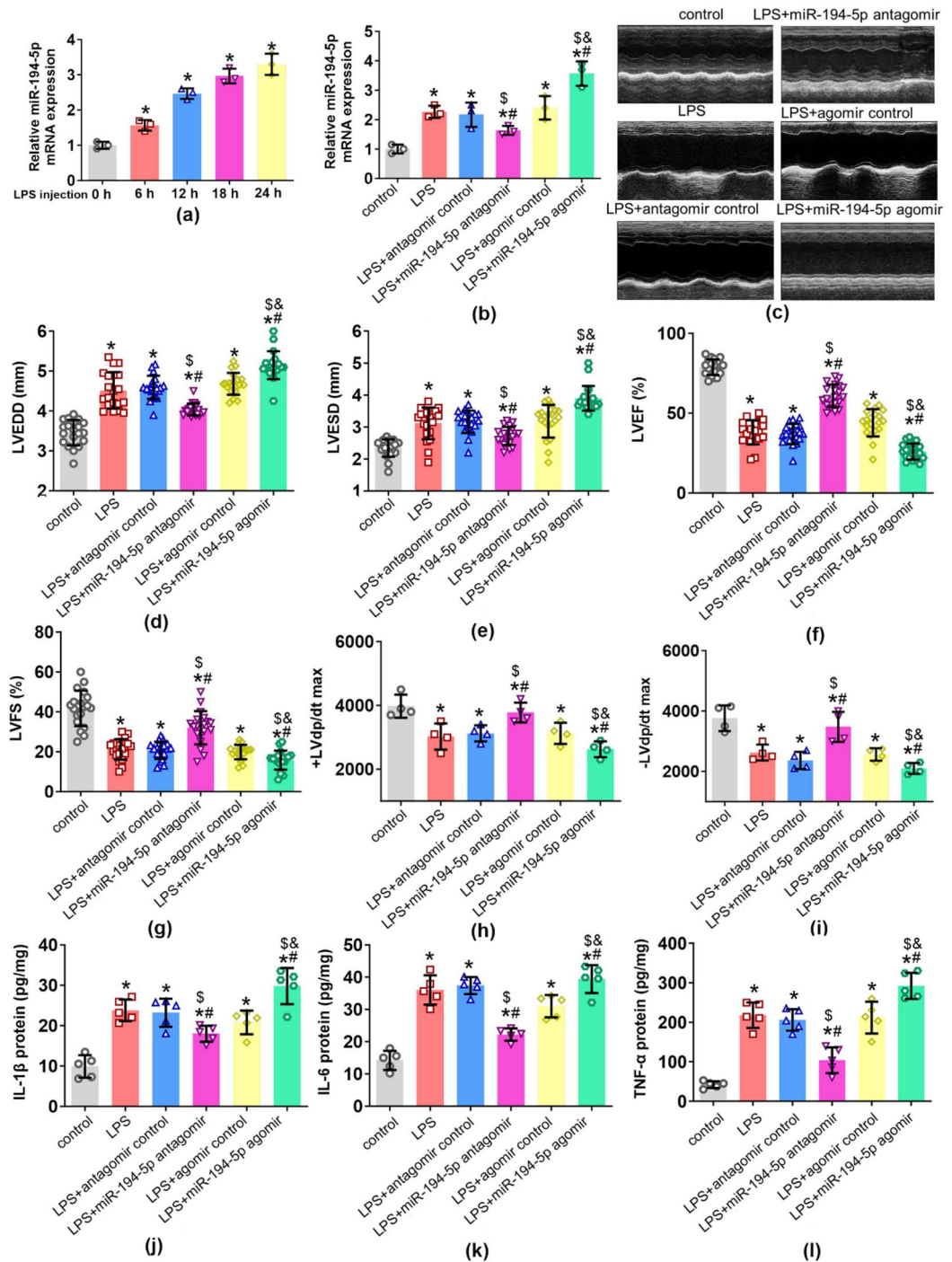


**Fig. 1.** Effects of miR-194-5p knockdown or overexpression on cardiac function and inflammation in mice with sepsis. **(a)** Levels of miR-194-5p mRNA expression in the septic myocardium at different time points after LPS injection (n = 3). \**P* < 0.05 versus 0 h. **(b)** Levels of miR-194-5p mRNA expression in the myocardium from the respective groups (n = 3). **(c)** Representative echocardiographic images (n = 20). **(d)** Left ventricular end-diastolic diameter (LVEDD). **(e)** Left ventricular end-systolic diameter (LVESD). **(f)** Left ventricular ejection fraction (LVEF). **(g)** Left ventricular fraction shortening (LVFS). **(h)** and **(i)** First derivative of the left ventricular pressure ( $\pm$  LV dp/dt max) (n = 4). **(j–l)** Levels of IL-1 $\beta$ , IL-6, and TNF- $\alpha$  in heart tissue were measured (n = 5). \**P* < 0.05 versus control, #*P* < 0.05 versus LPS, \$*P* < 0.05 versus LPS + antagomir control, &*P* < 0.05 versus LPS + agomir control.

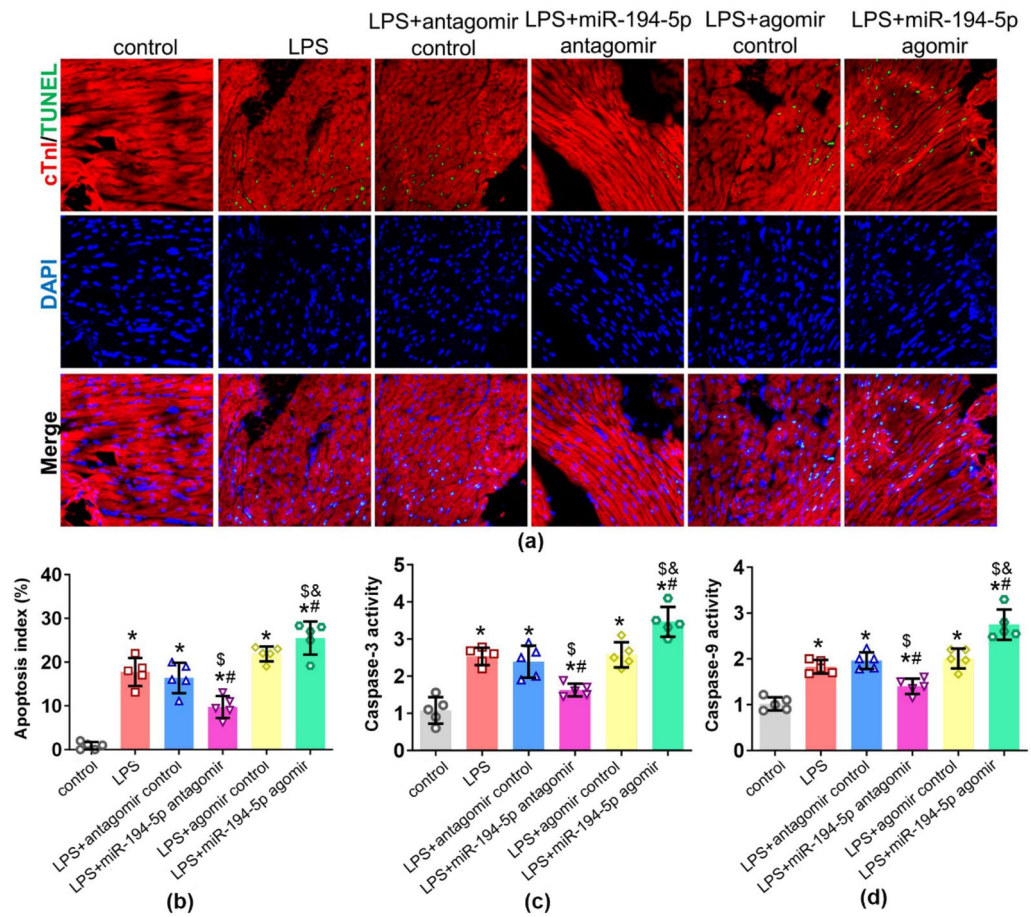


**Fig. 2.** Effects of miR-194-5p knockdown or overexpression on apoptosis in hearts from sepsis-challenged mice. **(a)** and **(b)** Representative immunofluorescence images of TUNEL (green), DAPI staining (blue), and Troponin I antibody staining (red) and quantification of TUNEL-positive cells (n = 5). **(c)** and **(d)** Caspase-3 and caspase-9 activities in heart tissue were measured (n = 5). \* $P < 0.05$  versus control, # $P < 0.05$  versus LPS, \$ $P < 0.05$  versus LPS + antagomir control, & $P < 0.05$  versus LPS + agomir control.

### MiR-194-5p antagomir relieves, whereas miR-194-5p agomir exacerbates mitochondrial dysfunction and oxidative stress in the septic myocardium

Mitochondrial dysfunction is involved in the occurrence and development of LPS-induced myocardial injury<sup>4</sup>. The effects of miR-194-5p inhibition or overexpression on mitochondrial ultrastructural changes were assessed by transmission electron microscopy (Fig. 3a). Mitochondria with sharply defined cristae lining up alongside the myofibrils were observed in the control myocardium. Swelling mitochondria with ruptured cristae, even accompanied by vacuolization of mitochondria were seen in the septic myocardium. Interestingly, miR-194-5p antagomir improved mitochondrial structural injury, but miR-194-5p agomir acted oppositely in the septic myocardium. Consistent with the morphological changes of mitochondria, decreased ATP content, CS activity and mCRC were detected in the septic myocardium compared with in the control myocardium, and treatment with miR-194-5p antagomir significantly increased the level of these three indexes. MiR-194-5p agomir treatment further decreased the ATP content, CS activity and mCRC in hearts from sepsis-challenged mice (Fig. 3b–d).

Oxidative stress exerts negative influence on SIC<sup>5</sup>. The levels of ROS and MDA were evaluated to investigate the effect of miR-194-5p inhibition or overexpression on oxidative stress in the septic myocardium (Fig. 3e,f). The levels of ROS and MDA were significantly increased in the septic myocardium compared with in the control myocardium. The levels of ROS and MDA were significantly decreased in the hearts of miR-194-5p antagomir-treated mice, while increased in miR-194-5p agomir-treated mice.

### DUSP9 is a direct target of miR-194-5p

Bioinformatics analysis was used to predict the biological function of miR-194-5p. As is shown in the workflow (Fig. 4a), target genes of miR-194-5p were predicted using miRDB ([www.mirdb.org](http://www.mirdb.org)), TargetScan (<http://www.targetscan.org>), and miRanda ([www.miranda.org](http://www.miranda.org)). A total of 178 targets were identified, and DUSP9 is a potential target. Increasing evidence indicates that DUSP9 is a key upstream regulatory molecule of MAPK signaling and dephosphorylation by DUSP9 manipulates the duration, intensity and spatiotemporal profile of the MAPK signaling cascade<sup>14,15</sup>. Thus, all predicted targets were used for pathway enrichment analysis. Based on the DAVID database, KEGG pathway<sup>19</sup> analysis indicates that the predicted targets were mostly enriched in

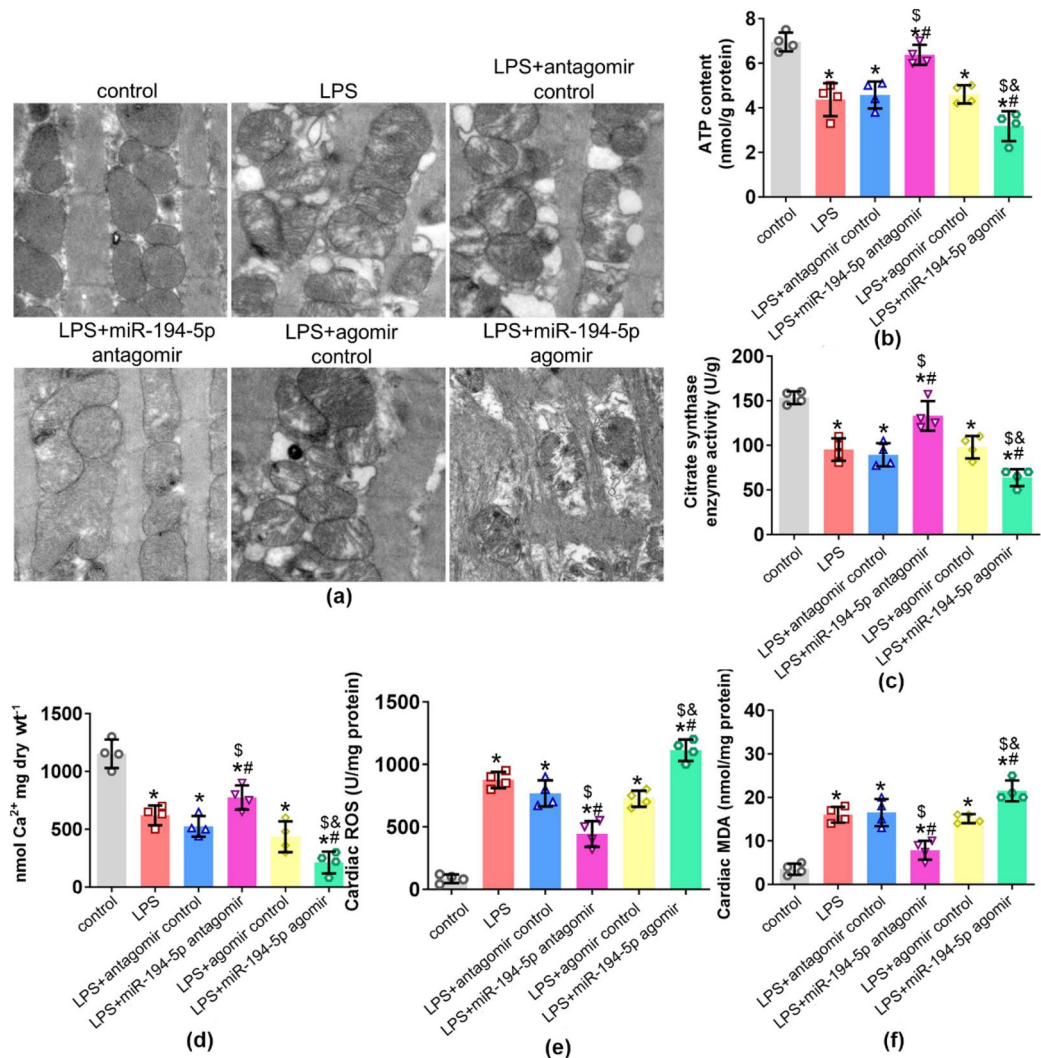


**Fig. 3.** Effects of miR-194-5p knockdown or overexpression on mitochondrial function and oxidative stress in hearts from sepsis-challenged mice. **(a)** Representative transmission electron micrographs of left ventricular specimens,  $n = 4$  in each group. **(b)** and **(c)** ATP content and citrate synthase (CS) in mitochondria isolated from mice,  $n = 4$  in each group. **(d)** Mitochondrial calcium retention capacity (mCRC),  $n = 4$  in each group. **(e)** and **(f)** Reactive oxygen species (ROS) and malondialdehyde (MDA) levels,  $n = 4$  in each group. \* $P < 0.05$  versus control, # $P < 0.05$  versus LPS, \$ $P < 0.05$  versus LPS + antagomir control, & $P < 0.05$  versus LPS + agomir control.

“MAPK signaling pathway” (Fig. 4b). Besides, DUSP9 plays a crucial role in cardiovascular disease<sup>14,15</sup>, so we selected this target for further investigation. As shown in Fig. 4c, DUSP9 3'-UTR contained the binding sequence of miR-194-5p. DUSP9-3'UTR or Mut-DUSP9-3'UTR reporter plasmids were co-transfected into HEK293T cells with or without miR-194-5p overexpression. The relative luciferase activity of DUSP9-3'UTR was significantly inhibited by miR-194-5p transfection. However, the mutant reporter plasmid invalidated the miR-194-5p mediated decrease in luciferase activity (Fig. 4d). These data indicate that DUSP9 is a potential target of miR-194-5p.

More and more studies have revealed that DUSP9 can repress the activation of p38 and JNK pathways by dephosphorylating serine/threonine and tyrosine residues<sup>14,15</sup>, whether miR-194-5p exerts an influence on the hearts of septic mice by targeting the DUSP9-p38/JNK axis is still unknown. Protein levels of DUSP9, p-p38, p38, p-JNK and JNK were measured at 0 h, 6 h, 12 h, 18 h and 24 h after LPS injection (Fig. 5a). Western blot analysis found a time-dependent downregulation in DUSP9 expression as well as upregulation in the protein levels of p-p38 and p-JNK in the septic myocardium (Fig. 5a–d). In addition, miR-194-5p depletion in the septic myocardium upregulated DUSP9 and downregulated p-p38 and p-JNK at the protein level, while miR-194-5p overexpression in the septic myocardium resulted in opposite results (Fig. 5e–h). These data indicate that miR-194-5p could promote the activation of p38 and JNK signaling pathways via targeting DUSP9 in the septic myocardium.

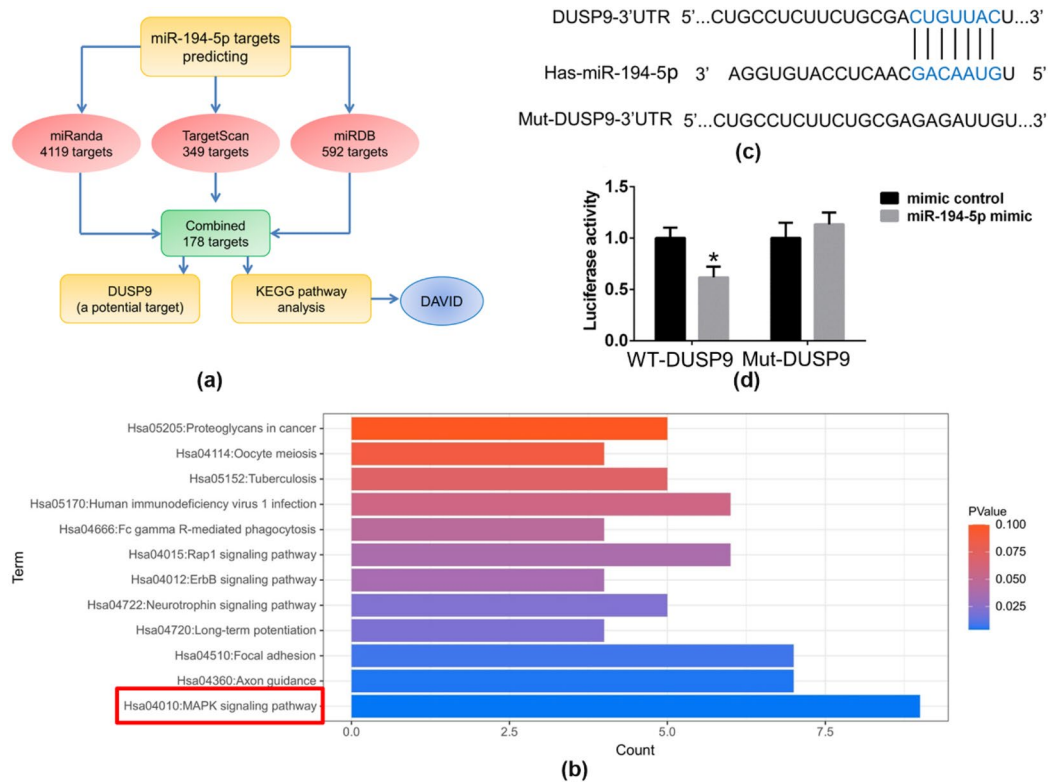


**Fig. 4.** DUSP9 was a direct target of miR-194-5p. **(a)** Workflow showing miR-194-5p target screening and the tools used for the KEGG pathway analysis. **(b)** DAVID KEGG analysis results for the predicted targets. The results were ranked by *P* value. **(c)** and **(d)** Luciferase reporter gene activity was used to detect the binding of miR-194-5p to the 3'UTR region or mutant 3'UTR region of DUSP9 mRNA. \**P* < 0.05 versus mimic control.

### DUSP9 inhibition ablated the protective effects of miR-194-5p antagomir on cardiac function and inflammation in mice with LPS-induced sepsis

To further demonstrate the important role of miR-194-5p/DUSP9 signaling in LPS-induced myocardial injury, we utilized AAV9 particles to explore whether blocking DUSP9 could reverse the benefits of miR-194-5p antagomir. Knockdown efficiency of shDUSP9-expressing AAV9 particles at the protein level in the septic myocardium was confirmed by western blot (Fig. 6a,b). Western blot analysis found a significantly decrease in DUSP9 expression as well as a significantly increase in protein levels of p-p38 and p-JNK in the LPS + shDUSP9 group compared with in the LPS + shCtrl group. Besides, DUSP9 depletion not only reduced DUSP9 expression but enhanced protein levels p-p38 and p-JNK in the hearts of miR-194-5p antagomir-injected septic mice (Fig. 6a–d).

Echocardiography showed that DUSP9 inhibition alone further decreased cardiac function markers LVEF, LVFS, LVSP, and  $\pm$  LV dp/dt and increased LVEDD, LVESD, and LVEDP in the septic mice. Additionally, DUSP9 inhibition ablated the protective effects of miR-194-5p antagomir on cardiac function as evidenced by increased LVEDD, LVESD, and LVEDP, and decreased LVEF, LVFS, LVSP, and  $\pm$  LV dp/dt in the miR-194-5p antagomir-injected septic mice (Fig. 6e–k; Supplement Fig. 3a,b). Consistent with the changes in heart function, DUSP9 depletion alone could contribute to an increase in levels of IL-1 $\beta$ , IL-6 and TNF- $\alpha$  in the hearts of septic mice. Furthermore, DUSP9 depletion reversed miR-194-5p antagomir-mediated suppression of inflammation as demonstrated by the increased levels of IL-1 $\beta$ , IL-6 and TNF- $\alpha$  in the hearts of miR-194-5p antagomir-injected septic mice (Fig. 6l–n). Besides, DUSP9 depletion enhanced p-p65 protein level in the hearts of miR-194-5p antagomir-injected septic mice, but not protein levels of p-Jak2 and p-Stat3 (Supplement Fig. 4a–d). These data indicate that inhibition of miR-194-5p avoids DUSP9 downregulation thus improving cardiac function and inhibiting inflammation in the septic myocardium.

### DUSP9 inhibition abolished the protective effects of miR-194-5p antagomir on cardiac apoptosis in septic mice

TUNEL assays showed that the silencing of DUSP9 alone further significantly increased TUNEL-positive cells and enhanced caspase-3 and caspase-9 activities in the LPS + shDUSP9 group compared with in the LPS + shCtrl group (Fig. 7a–d). Interestingly, the silencing of DUSP9 invalidated miR-194-5p antagomir mediated-apoptosis suppression and the downregulation of caspase-3 and caspase-9 activities in the hearts of miR-194-5p antagomir-injected septic mice (Fig. 7a–d), indicating that inhibition of miR-194-5p avoids DUSP9 downregulation thus reducing cardiac apoptosis in the septic myocardium.



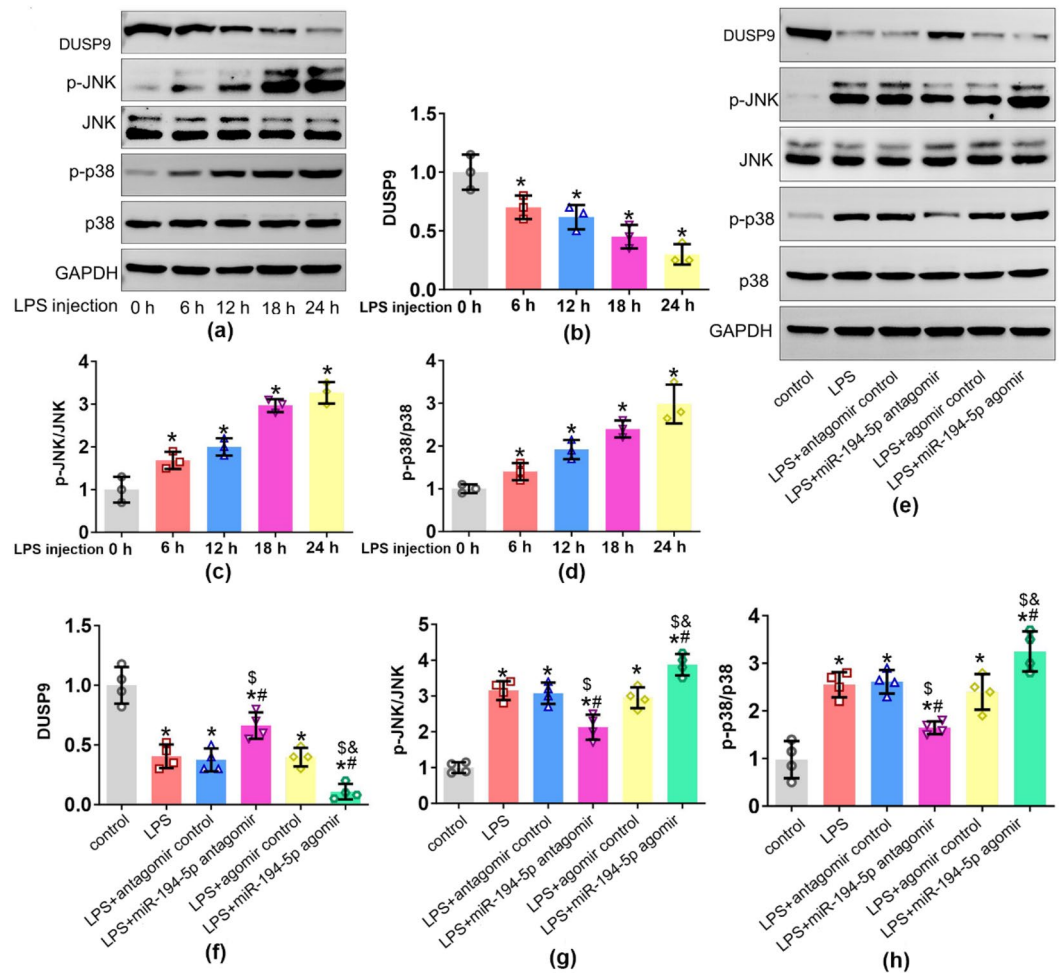


**Fig. 5.** Effects of miR-194-5p knockdown or overexpression on DUSP9-p38/JNK axis. (a–d) Representative immunoblots for DUSP9, p-p38, p-38, p-JNK, JNK and GAPDH in the septic myocardium at different time points after LPS injection and densitometric quantification ( $n = 3$ ).  $*P < 0.05$  versus 0 h. (e–h) MiR-194-5p depletion in the septic myocardium upregulated DUSP9 and downregulated p-p38 and p-JNK at the protein level, while miR-194-5p overexpression in the septic myocardium resulted in opposite results. Representative immunoblots for DUSP9, p-p38, p-38, p-JNK, JNK and GAPDH in the septic myocardium at different time points after LPS injection and densitometric quantification ( $n = 4$ ).  $*P < 0.05$  versus control,  $^{\#}P < 0.05$  versus LPS,  $^{\$}P < 0.05$  versus LPS + antagomir control,  $^{\&}P < 0.05$  versus LPS + agomir control.

### DUSP9 inhibition abolished the protective effects of miR-194-5p antagomir on mitochondrial dysfunction and oxidative stress in the septic myocardium

Transmission electron microscopy was used to assess the role of miR-194-5p/DUSP9 signaling in changes of mitochondrial ultrastructure (Fig. 8a). The results revealed that DUSP9 knockdown further caused damage to mitochondrial ultrastructure in the septic myocardium. Consistent with changes in mitochondrial ultrastructure, DUSP9 knockdown further significantly decreased ATP content, CS activity and mCRC in the LPS + shDUSP9 group compared with those in the LPS + shCtrl group. Interestingly, DUSP9 inhibition abolished the protective effects of miR-194-5p antagomir on mitochondria as evidenced by the ruptured and disappeared cristae in some mitochondria and the decreased ATP content, CS activity and mCRC in the hearts of miR-194-5p antagomir-injected septic mice (Fig. 8a–d). In addition, a significant upregulation in the levels of ROS and MDA was observed when comparing the hearts of shDUSP9-injected septic mice and shCtrl-injected septic mice. DUSP9 inhibition cancelled the protective effects of miR-194-5p antagomir on oxidative stress as evidenced by increased levels of ROS and MDA (Fig. 8e–f). These data indicate that inhibition of miR-194-5p avoids DUSP9 downregulation thus alleviating mitochondrial dysfunction and oxidative stress in the septic myocardium.

### Discussion

LPS is derived from the Gram-negative bacterium and considered as an essential pathogenic factor in the pathogenesis of sepsis<sup>20</sup>. LPS can activate immune cells and the immune system to induce a systemic inflammatory response, which can further lead to SIC<sup>20</sup>. SIC has generally been defined as an intrinsic and reversible systolic

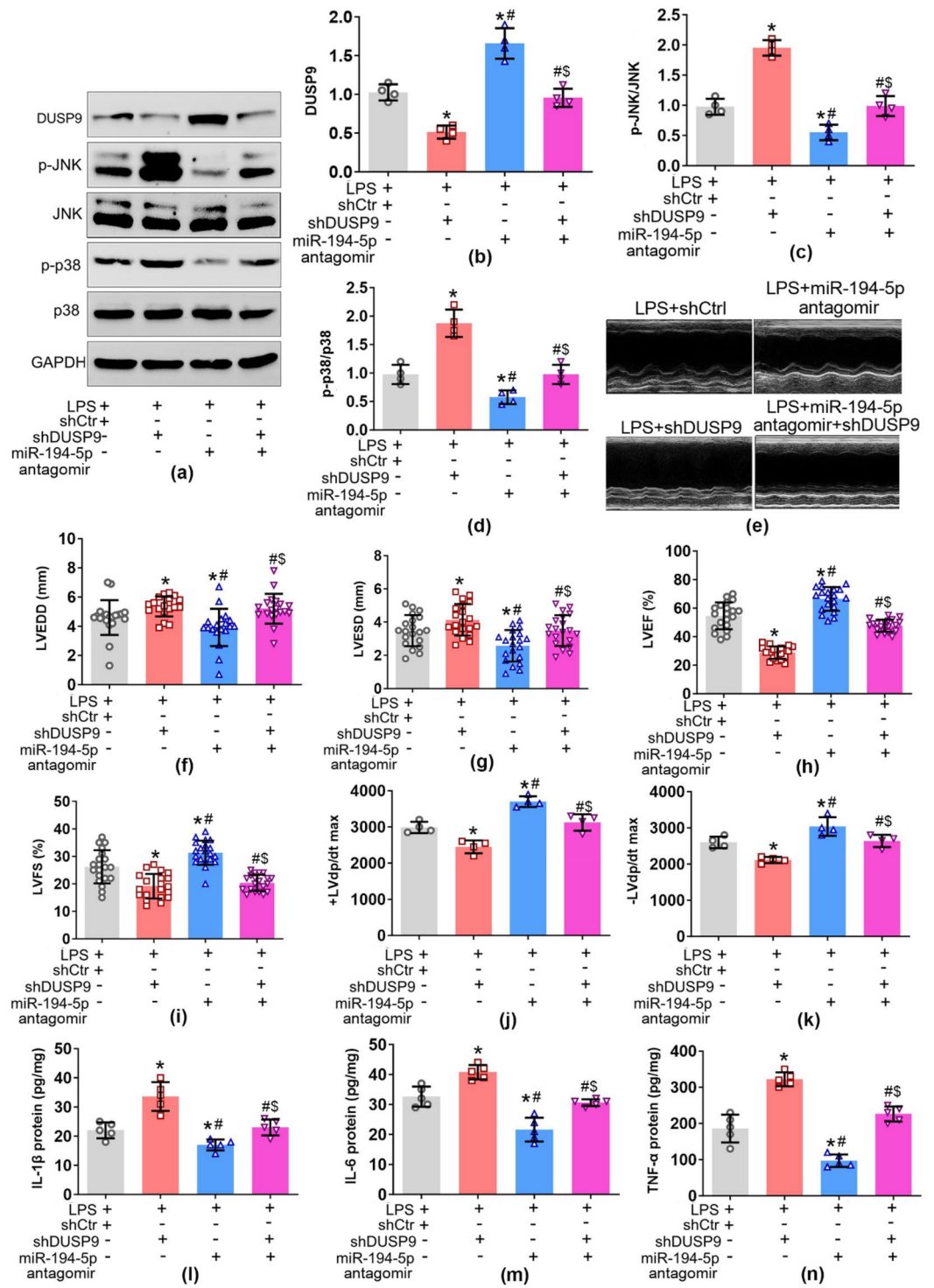


**Fig. 6.** DUSP9 inhibition abolished the favorable effects of miR-194-5p antagomir on cardiac function and inflammation in sepsis-challenged mice. **(a–d)** Representative immunoblots for DUSP9, p-p38, p-38, p-JNK, JNK and GAPDH in the heart tissue from the respective groups (n = 4). **(e)** Representative echocardiographic images are shown (n = 20). **(f)** Left ventricular end-diastolic diameter (LVEDD). **(g)** Left ventricular end-systolic diameter (LVESD). **(h)** Left ventricular ejection fraction (LVEF). **(i)** Left ventricular fraction shortening (LVFS). **(j)** and **(k)** First derivative of the left ventricular pressure ( $\pm$  LV dp/dt max) (n = 4). **(l–n)** Levels of IL-1 $\beta$ , IL-6, and TNF- $\alpha$  in heart tissue were measured (n = 5). \**P* < 0.05 LPS + shCtrl, #*P* < 0.05 versus LPS + shDUSP9, \$*P* < 0.05 versus LPS + miR-194-5p antagomir.

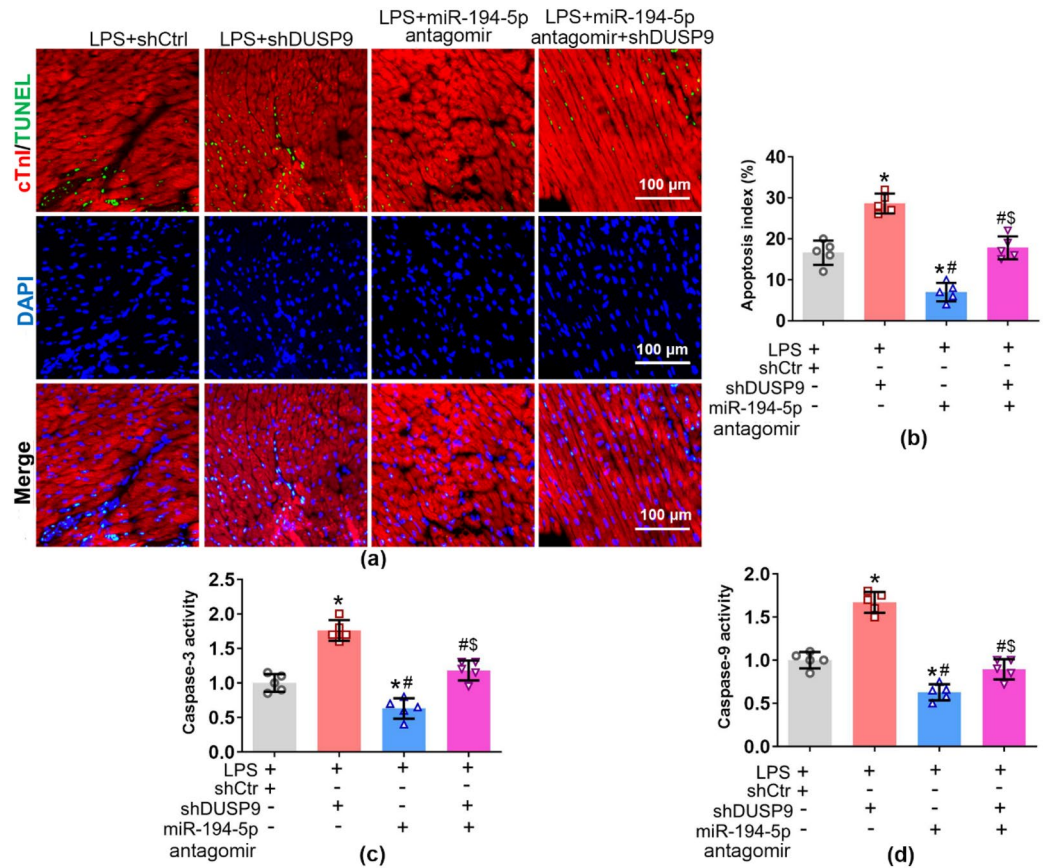


**Fig. 7.** DUSP9 inhibition blocked the effects of miR-194-5p antagonist on apoptosis in hearts from sepsis-challenged mice. **(a)** and **(b)** Representative immunofluorescence images of TUNEL (green), DAPI staining (blue), and Troponin I antibody staining (red) and quantification of TUNEL-positive cells (n = 5). **(c)** and **(d)** Caspase-3 and caspase-9 activities in heart tissue were measured (n = 5). \* $P < 0.05$  LPS + shCtrl, \* $P < 0.05$  versus LPS + shDUSP9,  $^{\$}P < 0.05$  versus LPS + miR-194-5p antagonist.

and diastolic dysfunction of both the left and right sides of the heart induced by sepsis<sup>1</sup>. Accumulating studies have reported that multiple miRNAs can exert crucial effects in various kinds of diseases. The potential clinical value of multiple miRNAs deserves deep exploration and finding effective miRNAs engaged in SIC may be an effective way to improve the strategies of SIC treatment in the future. MiR-194-5p has been proved to exert a critical role in a variety of diseases, including multiple types of tumors<sup>21–25</sup>, atopic dermatitis<sup>26</sup>, psoriasis<sup>27</sup>, chronic cerebral ischaemia<sup>28</sup>, intervertebral disc degeneration<sup>29</sup>, postmenopausal osteoporosis<sup>30</sup>, but the effects of miR-194-5p on SIC are barely elucidated. Our major finding in this study was that miR-194-5p antagonist mitigated sepsis-induced cardiac dysfunction, inflammation, apoptosis, mitochondrial dysfunction and oxidative stress in the hearts of septic mice, while miR-194-5p agomir triggered the opposite effect, indicating that miR-194-5p is detrimental in sepsis-induced cardiac injury. Furthermore, DUSP9 is a direct target of miR-194-5p and the cardioprotective effects of miR-194-5p antagonist were abolished through inhibiting DUSP9. Therefore, our results revealed that the miR-194-5p/DUSP9 pathway might serve as a potential therapeutic target for septic myocardial dysfunction.

Recently, miR-194-5p has been identified to be correlated with cardiovascular risk factors<sup>31</sup>. Additionally, the abnormal regulation of miR-194-5p has been revealed to play crucial roles in myocardial ischemia/reperfusion injury<sup>32</sup> and doxorubicin-induced cardiotoxicity<sup>13</sup>. But it is worth noting that the effects of miR-194-5p on cardiovascular injuries are controversial depending on different experimental models. Zhang et al.<sup>32</sup> found that the expression of miR-194-5p was decreased in myocardial ischemia/reperfusion-induced injury, and overexpression of miR-194-5p could improve cardiomyocyte damage in ischemic models. Conversely, Fa et al.<sup>13</sup> argued that miR-194-5p was upregulated in mouse heart tissue with doxorubicin treatment, and silencing miR-194-5p could alleviate DOX-induced cardiotoxicity. Thus it is urgently needed to make sense of the functional roles of miR-194-5p in sepsis-cardiac dysfunction. Interestingly, in the present study, pharmacological inhibition of miR-194-5p improved cardiac function in the hearts of septic mice as evidenced by decreased levels of LVEDD, LVESD, and LVEDP, and increased levels of LVEF, LVFS, LVSP, and  $\pm$  LV dp/dt, while overexpression of miR-194-5p further exacerbated cardiac dysfunction as demonstrated by the opposite changes in cardiac function markers.

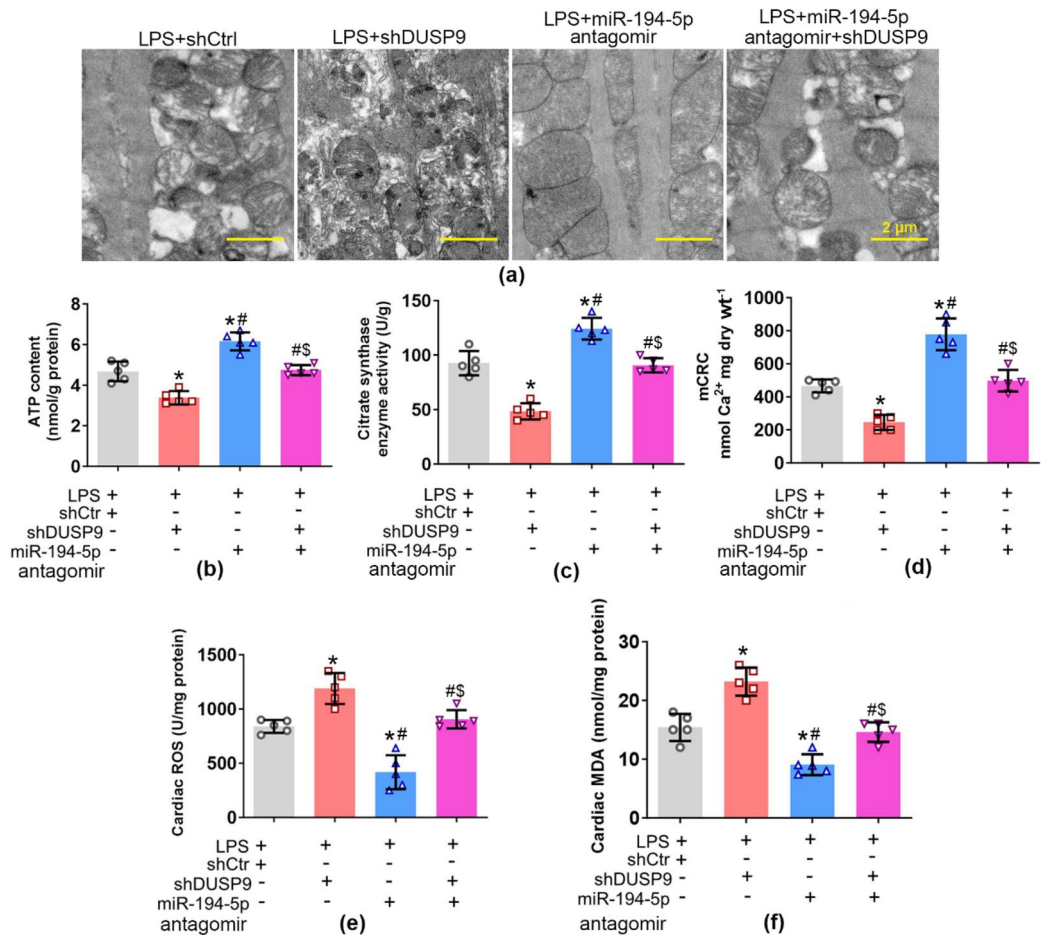


**Fig. 8.** DUSP9 inhibition hindered the effects of miR-194-5p antagonist on mitochondrial function and oxidative stress in hearts of sepsis-challenged mice. **(a)** Representative transmission electron micrographs of left ventricular specimens, n = 5 in each group. **(b)** and **(c)** ATP content and citrate synthase (CS) in mitochondria isolated from mice, n = 5 in each group. **(d)** Mitochondrial calcium retention capacity (mCRC), n = 5 in each group. **(e)** and **(f)** Reactive oxygen species (ROS) and malondialdehyde (MDA) levels, n = 5 in each group. \* $P < 0.05$  LPS + shCtrl, # $P < 0.05$  versus LPS + shDUSP9, \$ $P < 0.05$  versus LPS + miR-194-5p antagonist.

As a well-known immunomodulatory miRNA, miR-194-5p has been reported to be induced by LPS and control the inflammatory response in different cells and organs<sup>29,33–38</sup>. Notably, a recent study has revealed that miR-194a-5p could regulate the expression of Toll-like receptor 4 (TLR4), an important molecule involved in pathogen virulence, recognition and activation of innate immunity in *Salmonella* infection<sup>37</sup>. Besides, miR-194-5p has been reported to regulate the TRAF6/NLRP3 interaction and alleviate neuroinflammation in intracerebral hemorrhage<sup>35</sup>. However, the effect of miR-194-5p on inflammation in sepsis-induced myocardial dysfunction remains largely unclear. In the present study, we found that miR-194-5p antagonist significantly reduced the inflammatory factors IL-1 $\beta$ , IL-6 and TNF- $\alpha$  and decreased p-p65 expression in the septic myocardium, while miR-194-5p agomir further enhanced inflammatory factors IL-1 $\beta$ , IL-6 and TNF- $\alpha$  and increased p-p65 expression, indicating that regulation of inflammatory response may be one of the most important mechanisms for miR-194-5p antagonist to render myocardial protection to LPS-challenged mice.

Widespread cardiac apoptosis resulting in impaired cell activity is a crucial contributing factor to the development of SIC<sup>39</sup>. Enhanced cardiac apoptosis and caspase activity were detected in the hearts of septic rats, while inhibiting caspase activity improves cardiac function and apoptosis<sup>39</sup>. In the present study, miR-194-5p antagonist treatment decreased TUNEL-positive cells and caspase-3 and caspase-9 activities, whereas miR-194-5p agomir administration exerted an opposite role in the septic myocardium, indicating that caspase-9-mediated intrinsic apoptosis may be a crucial downstream pathway of miR-194-5p and mitochondria may greatly function in this process.

Therefore, the pathophysiological mechanisms of SIC through mitochondrial signaling are worth exploring. Sepsis-induced mitochondrial dysfunction contributing to SIC has been reported by a growing number of studies during sepsis, such as abnormalities in mitochondrial structure, mitochondrial energy metabolism disorder, oxidative stress, mitochondrial quality control systems and mitochondrial permeability transition<sup>40</sup>. In our study, we found that sepsis caused damage to mitochondrial structure and decreased the ATP content, CS activity and mCRC, consistent with previous findings<sup>40</sup>. Moreover, miR-194-5p antagonist treatment significantly ameliorated

the pathological abnormalities of mitochondria and increased the levels of the ATP content, CS activity and mCRC, while miR-194-5p agomir treatment further deteriorated mitochondrial structural injury and decreased the level of the ATP content, CS activity and mCRC in hearts from sepsis-challenged mice. Mitochondria are the primary source of ROS within cells under normal conditions<sup>40</sup>. Sepsis contributes to cardiac mitochondrial ROS formation and oxidative stress, resulting in mitochondrial damage and cardiac dysfunction, and simultaneously, sepsis-induced mitochondrial injury further promotes the generation of mitochondrial ROS<sup>41</sup>. In the present study, the levels of ROS and MDA were significantly decreased in the hearts of miR-194-5p antagomir-treated mice, while increased in miR-194-5p agomir-treated mice, indicating that the effects of miR-194-5p antagomir in SIC may be closely related to its ability to maintain a balance between oxidation and anti-oxidation, while miR-194-5p agomir disrupts this balance.

In this study, bioinformatics analysis was employed to screen putative targets of miR-194-5p. We identified that DUSP9 is a potential target and verified by a dual luciferase reporter assay. Interestingly, the KEGG pathway analysis was mainly enriched in “MAPK signaling pathway”. It is well known that DUSP9 has been reported to illustrate a substrate preference for the MAPK cascade, including JNK and p38 signaling pathways, both of which are related to the occurrence and development of cardiovascular diseases<sup>14,15</sup>. Therefore, miR-194-5p may exert its crucial effects in SIC by regulating DUSP9/MAPK axis. The present study documented time-dependent downregulation in DUSP9 expression as well as upregulation in the protein levels of p-p38 and p-JNK during the pathological development of sepsis-induced cardiac impairment. Moreover, upregulated DUSP9 protein level and downregulated protein levels of p-p38 and p-JNK were detected in the hearts of miR-194-5p antagomir-treated septic mice. In contrast, opposite results were observed in miR-194-5p agomir-treated septic mice. Furthermore, as expected, DUSP9 depletion reversed the inhibitory effect of miR-194-5p antagomir on levels of p-p38 and p-JNK. It abolished the protective effects of miR-194-5p antagomir on cardiac dysfunction, inflammation, apoptosis, mitochondrial dysfunction and oxidative stress in the hearts of septic mice. These findings indicate that inhibition of miR-194-5p avoids DUSP9 downregulation and further induces changes to MAPK-associated downstream proteins and signaling thus improving SIC.

However, there are still some limitations in the present study. Firstly, the effects of miR-194-5p inhibition or overexpression on cardiac dysfunction, inflammation, apoptosis, mitochondrial dysfunction and oxidative stress in SIC have not been verified with *in vitro* experiment. Secondly, whether miR-194-5p/DUSP9/MAPK axis has the same regulatory mechanisms in other cardiovascular disease models also deserves further substantiation. Besides, previous research has shown that miR-194-5p targets DUSP1, which is involved in the occurrence and development of SIC<sup>42–45</sup>. Thus, we cannot rule out the possibility that miR-194-5p can target other molecules involved in the progression of SIC. Despite these limitations, we believe that miR-194-5p plays a vital role in SIC development and miR-194-5p may be an important therapeutic target for SIC.

In conclusion, we have demonstrated that miR-194-5p could target DUSP9 and further activates p38 and JNK signaling pathways (Fig. 9), thereby inducing cardiac dysfunction, inflammatory response, apoptosis, mitochondrial dysfunction and oxidative stress in the hearts of septic mice. Although these data collectively indicate miR-194-5p as a therapeutic target for sepsis-induced heart injury, more researches are needed to explore the clinical value of miR-194-5p antagomir in protecting against SIC.

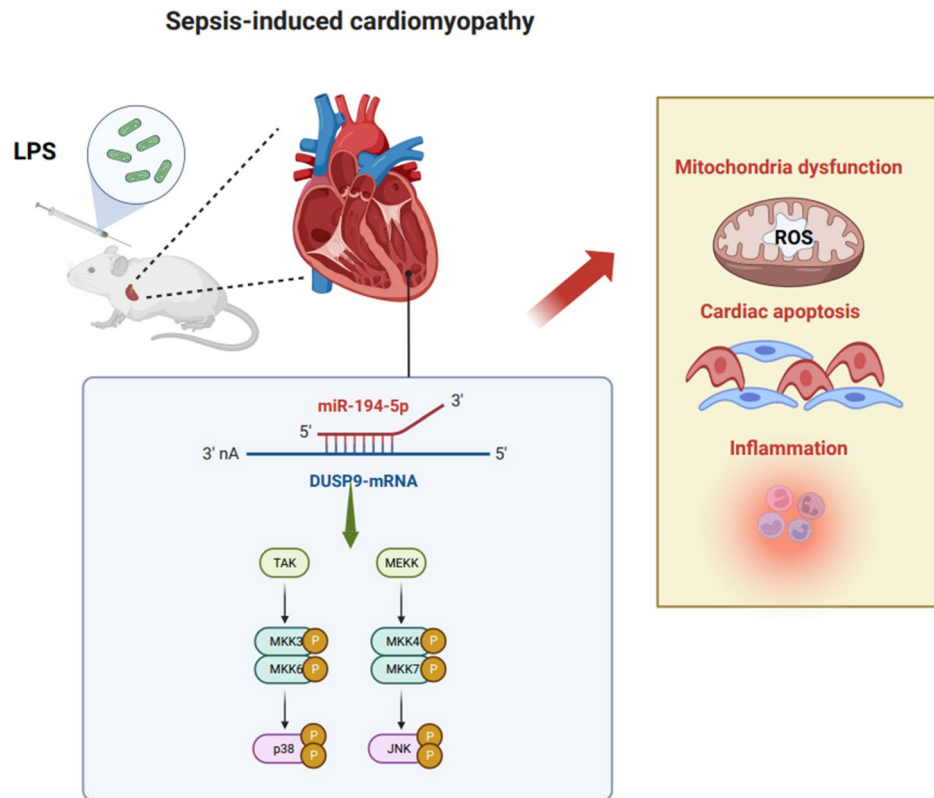


**Fig. 9.** A Schematic figure showed that miR-194-5p targeted DUSP9 and further activated p38 and JNK signaling pathways. It was created in BioRender (app.biorender.com) with license (WP275XTOTA).

### Data availability

The data that support the findings of this study are available from the corresponding authors upon request.

Received: 21 February 2024; Accepted: 26 August 2024

Published online: 02 September 2024

### References

1. Stanzani, G., Duchon, M. R. & Singer, M. The role of mitochondria in sepsis-induced cardiomyopathy. *Biochim. Biophys. Acta Mol. Basis Dis.* **1865**(4), 759–773 (2019).
2. Cheng, B., Hoefl, A. H., Book, M., Shu, Q. & Pastores, S. M. Sepsis: Pathogenesis, biomarkers, and treatment. *BioMed Res. Int.* **2015**, 846935 (2015).
3. Huang, M., Cai, S. & Su, J. The pathogenesis of sepsis and potential therapeutic targets. *Int. J. Mol. Sci.* **20**(21), 5376 (2019).
4. Yang, H. & Zhang, Z. Sepsis-induced myocardial dysfunction: The role of mitochondrial dysfunction. *Inflamm. Res. Off. J. Eur. Histamine Res. Soc.* **70**(4), 379–387 (2021).
5. Liu, Y. C., Yu, M. M., Shou, S. T. & Chai, Y. F. Sepsis-induced cardiomyopathy: Mechanisms and treatments. *Front. Immunol.* **8**, 1021 (2017).
6. Bhaskaran, M. & Mohan, M. MicroRNAs: History, biogenesis, and their evolving role in animal development and disease. *Vet. Pathol.* **51**(4), 759–774 (2014).
7. Shah, A. A., Meese, E. & Blin, N. Profiling of regulatory microRNA transcriptomes in various biological processes: A review. *J. Appl. Genet.* **51**(4), 501–507 (2010).
8. Pu, M. *et al.* Regulatory network of miRNA on its target: Coordination between transcriptional and post-transcriptional regulation of gene expression. *Cell. Mol. Life Sci.* **76**(3), 441–451 (2019).
9. Wojciechowska, A., Braniewska, A. & Kozar-Kaminska, K. MicroRNA in cardiovascular biology and disease. *Adv. Clin. Exp. Med. Off. Organ Wroclaw Med. Univ.* **26**(5), 865–874 (2017).
10. Vishnoi, A. & Rani, S. MiRNA biogenesis and regulation of diseases: An overview. *Methods Mol. Biol.* **1509**, 1–10 (2017).
11. Matsumoto, S. *et al.* Circulating p53-responsive microRNAs are predictive indicators of heart failure after acute myocardial infarction. *Circ. Res.* **113**(3), 322–326 (2013).
12. Nie, H., Pan, Y. & Zhou, Y. Exosomal microRNA-194 causes cardiac injury and mitochondrial dysfunction in obese mice. *Biochem. Biophys. Res. Commun.* **503**(4), 3174–3179 (2018).
13. Fa, H. *et al.* MicroRNA-194-5p attenuates doxorubicin-induced cardiomyocyte apoptosis and endoplasmic reticulum stress by targeting P21-activated kinase 2. *Front. Cardiovasc. Med.* **9**, 815916 (2022).
14. Khoubaï, F. Z. & Grosset, C. F. DUSP9, a dual-specificity phosphatase with a key role in cell biology and human diseases. *Int. J. Mol. Sci.* **22**(21), 11538 (2021).
15. Jiang, L. *et al.* Dual-specificity phosphatase 9 protects against cardiac hypertrophy by targeting ASK1. *Int. J. Biol. Sci.* **17**(9), 2193–2204 (2021).

16. Li, Y. *et al.* HOXA5-miR-574-5p axis promotes adipogenesis and alleviates insulin resistance. *Mol. Ther. Nucleic Acids* **27**, 200–210 (2022).
17. Wu, B. *et al.* Luteolin attenuates sepsis-induced myocardial injury by enhancing autophagy in mice. *Int. J. Mol. Med.* **45**(5), 1477–1487 (2020).
18. Gallo-Oller, G., Ordoñez, R. & Dotor, J. A new background subtraction method for Western blot densitometry band quantification through image analysis software. *J. Immunol. Methods* **457**, 1–5 (2018).
19. Kanehisa, M. & Goto, S. KEGG: Kyoto Encyclopedia of genes and genomes. *Nucleic Acids Res.* **28**(1), 27–30 (2000).
20. Naime, A. C. A., Ganaes, J. O. F. & Lopes-Pires, M. E. Sepsis: The involvement of platelets and the current treatments. *Curr. Mol. Pharmacol.* **11**(4), 261–269 (2018).
21. Wang, C. *et al.* miR-194-5p down-regulates tumor cell PD-L1 expression and promotes anti-tumor immunity in pancreatic cancer. *Int. Immunopharmacol.* **97**, 107822 (2021).
22. Xia, M. *et al.* MiR-194-5p enhances the sensitivity of nonsmall-cell lung cancer to doxorubicin through targeted inhibition of hypoxia-inducible factor-1. *World J. Surg. Oncol.* **19**(1), 174 (2021).
23. Liu, H. *et al.* MiR-194-5p inhibited metastasis and EMT of nephroblastoma cells through targeting Crk. *Kaohsiung J. Med. Sci.* **36**(4), 265–273 (2020).
24. Wang, Y. *et al.* MiR-194-5p inhibits cell migration and invasion in bladder cancer by targeting E2F3. *J. BUON Off. J. Balkan Union Oncol.* **23**(5), 1492–1499 (2018).
25. Wu, J., Zhang, L., Wu, S., Yi, X. & Liu, Z. miR-194-5p inhibits SLC40A1 expression to induce cisplatin resistance in ovarian cancer. *Pathol. Res. Pract.* **216**(7), 152979 (2020).
26. Meng, L. *et al.* Possible role of hsa-miR-194-5p, via regulation of HS3ST2, in the pathogenesis of atopic dermatitis in children. *Eur. J. Dermatol.* **29**(6), 603–613 (2019).
27. He, Q. *et al.* Circ\_0061012 contributes to IL-22-induced proliferation, migration and invasion in keratinocytes through miR-194-5p/GAB1 axis in psoriasis. *Biosci. Rep.* <https://doi.org/10.1042/BSR20203130> (2021).
28. Huang, K. *et al.* Effect of circular RNA, mmu\_circ\_0000296, on neuronal apoptosis in chronic cerebral ischaemia via the miR-194-5p/Runx3/Sirt1 axis. *Cell Death Discov.* **7**(1), 124 (2021).
29. Chen, Z. *et al.* Inflammation-dependent downregulation of miR-194-5p contributes to human intervertebral disc degeneration by targeting CUL4A and CUL4B. *J. Cell. Physiol.* **234**(11), 19977–19989 (2019).
30. Ding, H. *et al.* Medical examination powers miR-194-5p as a biomarker for postmenopausal osteoporosis. *Sci. Rep.* **7**(1), 16726 (2017).
31. Neiburga, K. D. *et al.* Vascular tissue specific miRNA profiles reveal novel correlations with risk factors in coronary artery disease. *Biomolecules* **11**(11), 1683 (2021).
32. Zhang, Q., Wu, X. & Yang, J. miR-194-5p protects against myocardial ischemia/reperfusion injury via MAPK1/PTEN/AKT pathway. *Ann. Transl. Med.* **9**(8), 654 (2021).
33. Yang, J. *et al.* Circular RNA CHST15 sponges miR-155-5p and miR-194-5p to promote the immune escape of lung cancer cells mediated by PD-L1. *Front. Oncol.* **11**, 595609 (2021).
34. Nan, C. C. *et al.* Knockdown of lncRNA MALAT1 alleviates LPS-induced acute lung injury via inhibiting apoptosis through the miR-194-5p/FOXO2 Axis. *Front. Cell Dev. Biol.* **8**, 586869 (2020).
35. Wan, S. Y. *et al.* MicroRNA-194-5p hinders the activation of NLRP3 inflammasomes and alleviates neuroinflammation during intracerebral hemorrhage by blocking the interaction between TRAF6 and NLRP3. *Brain Res.* **1752**, 147228 (2021).
36. Wang, M., Li, Z. & Zuo, Q. miR-194-5p inhibits LPS-induced astrocytes activation by directly targeting neurexophilin 1. *Mol. Cell. Biochem.* **471**(1–2), 203–213 (2020).
37. Herrera-Urbe, J. *et al.* Study of microRNA expression in *Salmonella* Typhimurium-infected porcine ileum reveals miR-194a-5p as an important regulator of the TLR4-mediated inflammatory response. *Vet. Res.* **53**(1), 35 (2022).
38. Zhang, C. *et al.* lncRNA MIR155HG accelerates the progression of sepsis via upregulating MEF2A by sponging miR-194-5p. *DNA Cell Biol.* **40**(6), 811–820 (2021).
39. Nevriere, R., Fauvel, H., Chopin, C., Formstecher, P. & Marchetti, P. Caspase inhibition prevents cardiac dysfunction and heart apoptosis in a rat model of sepsis. *Am. J. Respir. Crit. Care Med.* **163**(1), 218–225 (2001).
40. Lin, Y., Xu, Y. & Zhang, Z. Sepsis-Induced Myocardial Dysfunction (SIMD): The pathophysiological mechanisms and therapeutic strategies targeting mitochondria. *Inflammation* **43**(4), 1184–1200 (2020).
41. Lopes-Pires, M. E., Frade-Guanaes, J. O. & Quinlan, G. J. Clotting dysfunction in sepsis: A role for ROS and potential for therapeutic intervention. *Antioxidants* **11**(1), 88 (2021).
42. Hammer, M. *et al.* Dual specificity phosphatase 1 (DUSP1) regulates a subset of LPS-induced genes and protects mice from lethal endotoxin shock. *J. Exp. Med.* **203**(1), 15–20 (2006).
43. Tan, Y. *et al.* Dual specificity phosphatase 1 attenuates inflammation-induced cardiomyopathy by improving mitophagy and mitochondrial metabolism. *Mol. Metab.* **64**, 101567 (2022).
44. Liu, Z., Wang, J., Dai, F., Zhang, D. & Li, W. DUSP1 mediates BCG induced apoptosis and inflammatory response in THP-1 cells via MAPKs/NF- $\kappa$ B signaling pathway. *Sci. Rep.* **13**(1), 2606 (2023).
45. Lu, Y. *et al.* Integrative analysis of lncRNA-miRNA-mRNA-associated competing endogenous RNA regulatory network involved in EV71 infection. *Am. J. Transl. Res.* **13**(7), 7440–7457 (2021).

## Acknowledgements

This work was supported by the National Natural Science Foundation of China (Nos. 81900338 and 82000350). Figure 9 was created in BioRender (app.biorender.com) with license (WP275XTOTA).

## Author contributions

Q.H. and Z.J. designed the study. J.W. and T.W. performed the animal experiments; J.W., W.Z., Y.C., D.Z. and M.Z. completed the molecular experiments. J.H. participated in the data analysis; J.W. wrote the manuscript.

## Competing interests

The authors declare no competing interests.

## Additional information

**Supplementary Information** The online version contains supplementary material available at <https://doi.org/10.1038/s41598-024-71166-z>.

**Correspondence** and requests for materials should be addressed to Z.J. or Q.H.

**Reprints and permissions information** is available at [www.nature.com/reprints](http://www.nature.com/reprints).

**Publisher's note** Springer Nature remains neutral with regard to jurisdictional claims in published maps and institutional affiliations.

**Open Access** This article is licensed under a Creative Commons Attribution-NonCommercial-NoDerivatives 4.0 International License, which permits any non-commercial use, sharing, distribution and reproduction in any medium or format, as long as you give appropriate credit to the original author(s) and the source, provide a link to the Creative Commons licence, and indicate if you modified the licensed material. You do not have permission under this licence to share adapted material derived from this article or parts of it. The images or other third party material in this article are included in the article's Creative Commons licence, unless indicated otherwise in a credit line to the material. If material is not included in the article's Creative Commons licence and your intended use is not permitted by statutory regulation or exceeds the permitted use, you will need to obtain permission directly from the copyright holder. To view a copy of this licence, visit <http://creativecommons.org/licenses/by-nc-nd/4.0/>.

© The Author(s) 2024